

Modeling and Simulation of Down Draft Wood Gasifier

¹S. Siva Kumar, ¹K. Pitchandi and ²E. Natarajan

¹Department of Mechanical Engineering, College of Engineering, Anna University, Chennai-25, India

²Institute for Energy Studies, College of Engineering, Anna University, Chennai-25, India

Abstract: The conversion of biomass by gasification into a fuel suitable for use in a gas engine increases greatly the potential usefulness of biomass as a renewable resource. Gasification is a robust proven technology that can be operated either as a simple, low technology system based on a fixed-bed gasifier, or as a more sophisticated system using fluidized-bed technology. Hence there is huge expectation from the user industry for its application. For a country like India with its vast agricultural residues, there is a large requirement for an efficient power generation system. The critical operating parameters that affect the gasifier performance are wood diameter, air temperature, moisture content throat angle and throat diameter of fixed gasifier geometry. In the present study, mathematical model was developed to characterize the gasification performance of a typical biomass downdraft gasifier and the validated model is used to simulate the parametric study.

Key words: Gasifiers, gasification, pyrolysis

INTRODUCTION

Gasifiers are viable alternative for producing heat and power with minimal adverse impact on the environment. The gasification technology is now considered to be in an advanced stage of development. Hence there is huge expectation from the user industry for its application. For a country like India with its vast agricultural residues, there is a huge requirement for an efficient power generation system. Gasification is a high temperature chemical process in which solid fuel is reacted with a limited supply of air or oxygen to completely convert all the carbonaceous material into a fuel gas. Thus, thermo chemical characteristics of biomass play a major role in the selection of the gasification system design and performance (Iyer *et al.*, 2002).

In order to use the energy resources efficiently and economically, fast and quick simulation techniques with well-developed mathematical models are necessary. The critical operating parameters that affect the gasifier performances are wood diameter, moisture content, air temperature, throat angle and throat diameter of fixed gasifier geometry (Reed and Das, 1988). In the present study, mathematical model was developed to characterize the gasification performance of a typical biomass downdraft gasifier and the validated model is used to simulate the parametric study.

DOWN-DRAFT GASIFIERS

Figure 1 shows the major constructional features of a downdraft gasifier. In the region nearest the air inlet,

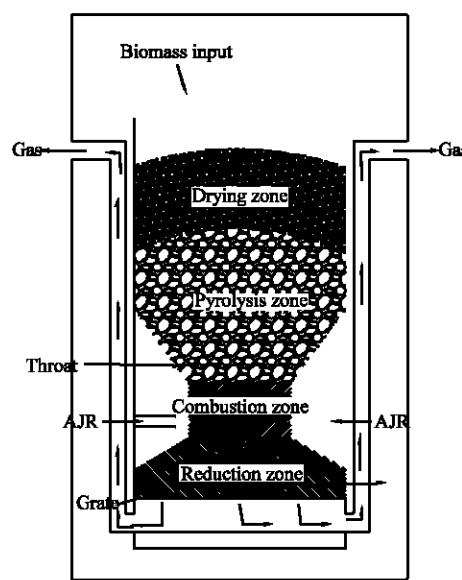


Fig. 1: Downdraft gasifier

flaming pyrolysis processes occur. Highly exothermic combustion reactions provide the energy to pyrolyse the solid fuel and these two processes can occur nearly simultaneously. The temperature in the flaming pyrolysis region is sufficiently high to thermally crack the pyrolysis products into components of low molecular weight. Down-draft gasifiers have relatively low tar content and therefore usually are the preferred type for small scale power generation from biomass, having said this, it should also be realized that the tar from down-draft gasifiers is more stable than from up-draft gasifiers, which

may still provide problems in tar removal. Downdraft gasification is a comparatively cheap method of gasification that can produce a product gas with very low tar content.

Moreover, proper operation asks for narrow specifications of both fuel size and moisture content (typically 20 wt % db). Further, the classical downdraft gasifier with its typical throat cannot be scaled-up. Even with special designs, such as a rotating cone in the throat (Groeneveld and Van Swaaj, 1979) to increase its efficiency, its maximum size, probably is limited to about 1 MWe.

MODELLING OF THE REDUCTION ZONE

Modeling the reduction zone is performed by following a char particle along the axis of reactor. In the mathematical representation of this zone, a small time increment approach is used since a continuous approach is not possible. This approach involves the use of a stepwise procedure starting at the reduction zone and marches longitudinally through the reactor in appropriate time increments. The input values at the first time interval are the output values from the flaming pyrolysis zone. The end of the reduction zone is reached when the particle carbon concentration in any location is less than a prescribed magnitude, usually 2 to 5% of the initial char concentration. The model formulation at any time step, Δt , is given as follows:

Superficial gas velocity: The superficial gas velocity is calculated using:

$$N_g = C_g V_g \tag{1}$$

$$C_g = \frac{P}{RT_g} \tag{2}$$

Total mole flux:

$$N_g = \frac{4 \times x_{gi} \times m_{fuel}}{\pi * D_t^2} \tag{3}$$

Combination of Eq. 1 and 2 results in

$$V_g = \frac{RT_g}{P} (N_{CO} + N_{H_2} + N_{H_2O} + N_{CO_2} + N_{CH_4} + N_{N_2}) \tag{4}$$

Concentrations of CO₂ and H₂O:

The bulk CO₂ Concentration = $C_{CO_2,b} = \frac{N_{CO_2}}{V_g \times e_b}$

The bulk H₂O Concentration = $C_{H_2O,b} = \frac{N_{H_2O}}{V_g \times e_b}$

$$(e_b) = 0.5 - \frac{0.2[r_p - r_o]}{r_p} \tag{5}$$

The void fraction, as reported by Perry *et al.* (1984), depends on the ratio of wood particle to reactor diameters and is in general confined within a range from 0.3 to 0.6 for various packings. In this context, it is proposed that the bed void fraction e_b varies from 0.3 to 0.5 depending on the particle diameter.

Mass transfer coefficients: The mass transfer coefficients for CO₂ and H₂O is are calculated (Sherwood *et al.*, 1975) from the equation:

$$K_{mCO_2} = \frac{1.17 \times Re_{CO_2}^{0.585} \times Sc_{CO_2}^{0.333} \times D_{CO_2}}{2r_o} \tag{6}$$

$$K_{mH_2O} = \frac{1.17 \times Re_{H_2O}^{0.585} \times Sc_{H_2O}^{0.333} \times D_{H_2O}}{2r_o} \tag{7}$$

Reynolds number (Re)

$$Re = \frac{2 \times V_o \times G}{Nm} \tag{8}$$

Schmidt number (Sc)

$$Sc \text{ for } CO_2 = Sc_{CO_2} = \frac{\mu}{\rho \times [D_{CO_2,m}]} \text{ or } \left(\frac{\mu}{\rho DA} \right) \tag{9}$$

$$Sc \text{ for } H_2O = Sc_{H_2O} = \frac{\mu}{\rho \times [D_{H_2O,m}]} \tag{10}$$

The superficial mass velocity is computed by summing the product of mole flux and molecular weight for all components, while the gas density is obtained by dividing the mass velocity by the gas velocity. (Goodridge and Quazi, 1967)

$$G = \sum_{i=1}^6 N_{g_i} \times M_{g_i} \tag{11}$$

$$\rho = \frac{\text{mass velocity}}{\text{gas velocity}} = \frac{G}{V_g} \tag{12}$$

Molecular diffusivity of component A to the mixture are calculated as follows:

$$D_{Am} = \frac{1 - Y_{gi}}{\sum_{\substack{j=1 \\ j \neq i}}^N \frac{Y_{gj}}{D_{ij}}} \quad (13)$$

Molecular diffusivity of component CO₂ to the mixture is:

$$D_{CO_2m} = \left[\frac{1 - Y_{CO_2}}{\frac{Y_{CO}}{K_{CO_2:CO}} + \dots + \frac{Y_{N_2}}{K_{CO_2:N_2}}} \right] \times T_g^{1.5}$$

The diffusivities of CO₂ and H₂O in the gas mixture are calculated according to Wilke's formulation as in Eq. 13.

The expression for viscosity of the fluid mixture (μ_m), as developed by Wilke (1950) is:

$$\mu_m = \sum_{i=1}^6 \left(\frac{\mu_i}{1 + \left(\frac{1}{Y_i} \right) \sum_{j=1}^6 Y_j \sum_{ij}} \right) \quad (14)$$

$$\sum_{ij} = \frac{1 + \left(\frac{\mu_j}{\mu_i} \right)^{0.5} \left(\frac{m_j}{m_i} \right)}{\sqrt{8 \times \left(1 + \frac{m_i}{m_j} \right)}} \quad (15)$$

Heat transfer coefficient: Heat transfer coefficient is calculated using the following empirical correlation developed by Petrovic and Thodos (1968) and Eckert (1956).

$$J_H = \frac{0.357}{Re^{0.359} \times \epsilon_b} \quad (16)$$

Heat transfer coefficient between solid and bulk fluid are (Colburn, 1931)

$$h = \frac{J_H \times C_p \times G}{Pr^{0.667}} \quad (17)$$

The thermal conductivity of the gas mixture, k_m , may be most conveniently calculated from component

conductivity values as in Perry *et al.* (1984). Chen (1987) has quoted from Friend and Adler (1958) that the thermal conductivity of the gas mixture can be calculated using the following equations.

$$K_m = \frac{\sum Y_i k_i (M_i)^{0.333}}{\sum Y_i (M_i)^{0.333}} \quad (18)$$

The mixture heat capacity is determined by summing the product of C_p and the mole fraction of each component. The component specific heat is obtained by taking the derivative of the enthalpy correlations with respect to temperature.

$$C_p = 8.134 \left[a_m + b_m T + c_m T^2 + d_m T^3 + e_m T^4 \right] \text{ kJ/kmol k}$$

$$a_m = Y_{CO_2} a_{CO_2} + Y_{H_2O} a_{H_2O} + Y_{CO} a_{CO} + Y_{H_2} a_{H_2} + Y_{CH_4} a_{CH_4} + Y_{N_2} a_{N_2}$$

Similarly, the values of b_m, c_m, d_m, e_m are calculated using Table 1.

Mass and heat transfer between solid surface and bulk:

The concept of gasification of char particle will be used here to calculate the temperature profile and the concentration in the particle. From these profiles the mass and heat fluxes (N) flowing into the particle can be determined. They can be written as follow:

$$N_{CO_2,s} = K_{mCO_2} (C_{CO_2,b} - C_{CO_2,s}) \quad (19)$$

$$N_{H_2O,s} = K_{mH_2O} (C_{H_2O,b} - C_{H_2O,s}) \quad (20)$$

$$N_{Heat,s} = h(T_b - T_s) \quad (21)$$

Based on the particle surface, the production of CO and H₂ are computed by:

$$N_{CO,s} = N_{H_2O,s} + 2N_{CO_2,s} \quad (22)$$

$$N_{H_2,s} = N_{H_2O,s} \quad (23)$$

Table 1: Calculated values of a_m, b_m, c_m, d_m, e_m

Gas composition	a	b	c	d	e
CH ₄	3.826	-3.979	24.558	-22.733	6.963
CO ₂	2.401	8.735	-6.607	2.002	0.000
H ₂ O	4.070	-1.108	4.152	-2.964	0.807
CO	3.710	-1.619	3.692	-2.032	0.240
H ₂	3.057	2.677	-5.180	5.521	-1.812
N ₂	3.675	-1.208	2.324	-0.632	-0.226

Converting these fluxes using reactor cross sectional area requires an expression of particle flux. This particle flux is represented as:

$$N_p = \frac{N_{Char}}{V_p * C_C} \quad (24)$$

The number of particles per unit cross-sectional area (n_p) during the given time step and the total particle surface, A_{pT} , are:

$$n_p = N_p \times \Delta t$$

$$\text{Single particle surface area } (A_{pT}) = n_p \times A_p \quad (25)$$

The component molar fluxes based on reactor cross section area can be deduced as follows.

$$N_{CO} (i) = N_{CO} (i-1) + N_{CO,S}A_{pT} \quad (26)$$

$$N_{H_2} (i) = N_{H_2} (i-1) + N_{H_2,S}A_{pT} \quad (27)$$

$$N_{CO_2} (i) = N_{CO_2} (i-1) - N_{CO_2,S}A_{pT} \quad (28)$$

$$N_{H_2O} (i) = N_{H_2O} (i-1) - N_{H_2O,S}A_{pT} \quad (29)$$

$$N_C (i) = N_C (i-1) - (N_{CO_2,S} + N_{H_2O,S})A_{pT} \quad (30)$$

Where:

i = Current time step

$i-1$ = Previous time step

However, the mole fluxes of N_2 , CH_4 and trace components remain unchanged.

Particle velocity and traveling distance: The distance that the particle travels during a given time step is calculated from the average velocity expressed as follows:

$$V_p = \frac{N_C (i) + N_C (i-1)}{C_{C,avg} \times (1 - \epsilon_b)} \quad (31)$$

Where:

$N_{C, avg} = N_C(i) + N_C(i-1)$ which is average mole flux of carbon

$C_{c,avg}$ = Average carbon concentration of the particle

The distance, ΔL , of particle traveling is determined by the following expression

$$\Delta L = V_p \times \Delta t \quad (32)$$

Determination of the current particle position is done by summing the individual values of ΔL starting from the inlet of the reduction zone.

Water gas shift reaction: The mole fluxes of N_2 , CH_4 and traces remain unchanged. The amount of shift (w_s) to restore the equilibrium is calculated from the equilibrium constant of the water-gas shift reaction. The equations are as follows.

$$K_3 = \frac{N_{CO_2} (i) + w_s)(N_{H_2} (i) + w_s)}{N_{CO} (i) - w_s)(N_{H_2O} (i) - w_s)} \quad (33)$$

Zainal (2002) has given the correlation between the temperature and equilibrium constant (K_3) for the water gas shift reaction in empirical formula as follows.

$$\ln k_3 = -36.72508 + \frac{3994.704}{T} - (4.46241 \times 10^{-3} T) + 6.71814 \times 10^{-7} T^2 + 12.22028 \ln T \quad (34)$$

So the final fluxes leaving the time step I are as follows:

$$N_{CO,e} = N_{CO} (i) - w_s \quad (35)$$

$$N_{H_2,e} = N_{H_2} (i) + w_s \quad (36)$$

$$N_{CO_2,e} = N_{CO_2} (i) + w_s \quad (37)$$

$$N_{H_2O,e} = N_{H_2O} (i) - w_s \quad (38)$$

Gaseous phase temperature: The gas phase temperature at the end of time step i is computed from a heat balance on solid and gas. The overall heat balance at the time step i can be written as:

$$(H_{gas} + H_{solid})_i + \Delta H_3 w_s = (H_{gas} + H_{solid})_e + H_{g-s} \quad (39)$$

H_{g-s} represents the heat flux transferred from the gas bulk into the solid particle and is numerically calculated as Yoon *et al.* (1978)

$$H_{g-s} = (T_b - T_s) A_{pT} \quad (40)$$

$$\Delta H_3 = -40.5 \text{ kJ kmol}^{-1}$$

Where:

i = Inlet condition

e = Exit condition

A computer programme has been formulated using C language to calculate the characteristic profiles along the reactor axis. The profile includes temperature, concentrations, efficiency and distance of the particle traveled.

PARAMETRIC STUDY OF REDUCTION ZONE SUB-MODEL

A set of computer simulations have been conducted to investigate the effects of operating parameters such as wood diameter, preheating of air, moisture content and design parameters such as throat angle and throat diameter on cumulative conversion efficiency. Chen (1987) mentioned that higher inlet air temperature is beneficial for cumulative conversion efficiency but the cost of this benefit needs to be investigated. Throat angle is a special unique feature of downdraft gasifiers and the effect of this on cumulative conversion efficiency is important. Table 2 presents the values of the parameters used for this study.

Temperature along the reduction zone: Gasification is mostly completed within a short distance below the end of the oxidation zone, because of the high temperature promoting fast reaction rates. The initial fast reactions, in conjunction with rapid heat consumption, result in a steep bulk temperature decline as shown in Fig. 2. Further temperature decreases in slower rate because of the slow reaction rates and the increasing molar rate in the bulk stream. A similar result was obtained by Yoon *et al.* (1978) in simulating the counter-current moving bed coal gasifier.

The effect of moisture content: Figure 3 shows the effect of moisture content on cumulative conversion efficiency for a wood diameter of 3 cm diameter. Moisture contents have a very important influence on the cumulative conversion efficiency and the reactor design requirement. As the moisture content increases, the cumulative conversion efficiency drops considerably for a constant gasifier location. Furthermore, the reactor length extends drastically to achieve a fixed conversion of 61% or higher. However, at lower conversions the moisture content has only a smaller effect. This observation is explained by the reaction kinetics. At a higher moisture content, the low oxidation temperature repressing the reaction rate is compensated by a high H₂O concentration which promotes the reaction (Parikh *et al.*, 1989). Thus, the variation in conversion is not severe. However, low bulk fluid temperature, caused by further reaction, tends to dominate the reaction rate and forces the Conversion to slow down.

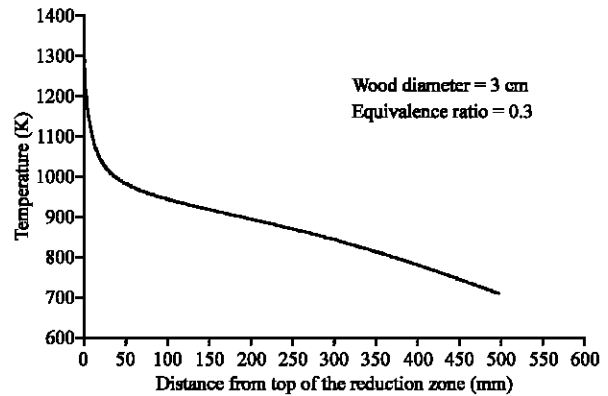


Fig. 2: Axial variation of temperature

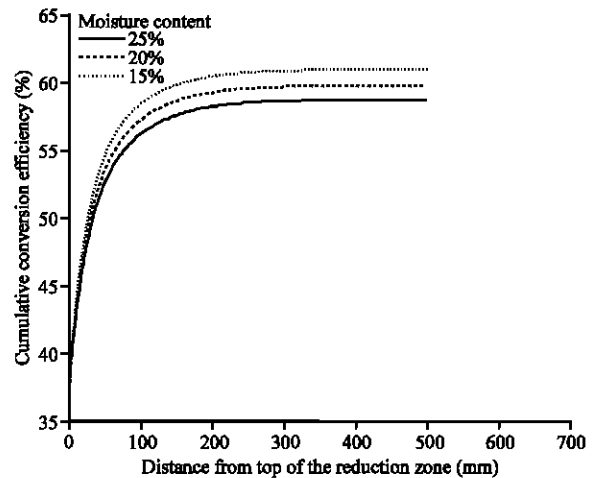


Fig. 3: Axial variation of cumulative conversion efficiency for different moisture content

Table 2: Parameters used for this study

Parameter	Range
Moisture content (%)	15, 20, 25
Wood diameter (cm)	1 - 6
Air temperature (K)	300 - 600
Throat angle (°)	45 - 90
Throat diameter (cm)	10- 30

The effect of wood diameter: The variation of cumulative conversion efficiency along the reduction zone for different wood diameter are shown in Fig. 4. It can be seen from this figure that as the wood diameter increases the length of the reduction zone must also increase before the conversion reaches its maximum. Thus larger wood diameter needs longer reactor lengths to achieve the maximum conversion. Char conversion consists of two processes namely, fast conversion and slow conversion. Fast conversion of char takes place at the entrance of the reduction zone due to the fast reaction rate (Jayah *et al.*, 2003). Smaller wood diameters are more likely to get

converted to gases completely before the slow conversion begins because of their size and fewer diffusion limitations during the reaction process. Thus gasifiers with shorter reactor lengths need small wood size. With the same environmental conditions, larger wood size also undergoes the same fast conversion but because of their size, complete conversion may not be possible. Larger wood chips undergo the remaining slow conversion and thus need a longer reactor length prior to leaving the reduction zone. As a result of faster char conversion, smaller wood chip size increase the cumulative conversion efficiency compared to larger chips (Milligan, 1994).

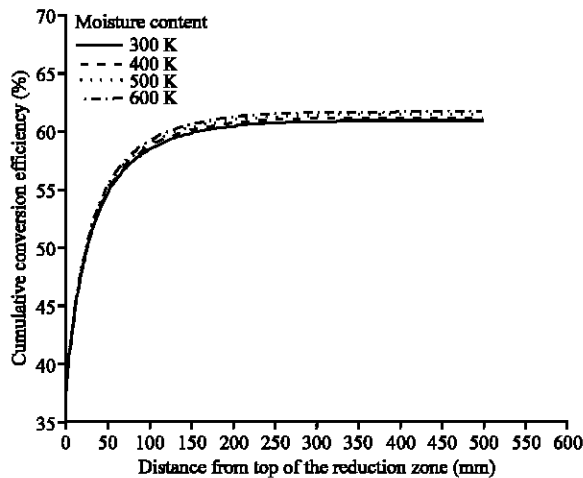


Fig. 4: Axial variation of cumulative conversion efficiency for different wood diameter

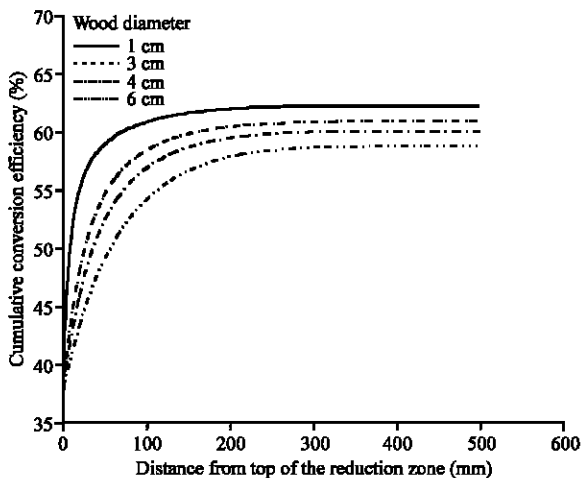


Fig. 5: Axial variation of cumulative conversion efficiency for different air temperature

The effect of preheating of air: Gasifiers are generally operated using ambient air at 300 K. But Fig. 5 shows the effect of preheating of air in the gasifier. Cumulative conversion efficiency increases as the inlet air temperature increases because hot air provides additional enthalpy necessary for reaction thereby decreasing the equivalence ratio. The cumulative conversion efficiency increases from 57.5 to 61% when the air temperature increases from 300 to 600K. It appears that the increase in cumulative conversion efficiency is not economical when compared to the amount of energy needed to raise the temperature of preheated air.

The effect of throat angle: Figure 6 shows the variation of cumulative conversion efficiency along the reduction zone axis for throat angles of 45 and 90 degree. The smaller angles (45 degree) tend to increase the cumulative conversion efficiency whereas larger angles (90 degree) decrease the cumulative conversion efficiency, because the latter decreases the temperature due to the divergent effect and hence the reaction rate. Although smaller angles increase the cumulative conversion efficiency, it also needs a longer reduction zone length to reach a higher efficiency. The effect of throat angles is not significant until the conversion process reaches the reduction zone length of 10 cm.

The effect of throat diameter: Figure 7 shows the variation of cumulative conversion efficiency along the reduction zone axis for throat diameter of 10, 20 and 30 cm. The smaller throat diameter (10 cm) tends to increase the cumulative conversion efficiency whereas larger

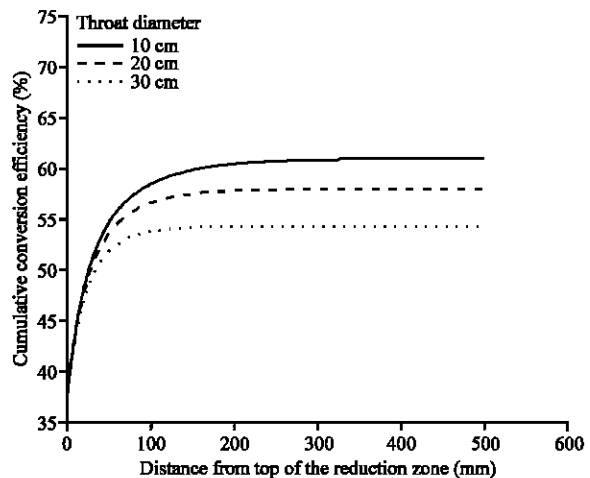


Fig. 6: Axial variation of cumulative conversion efficiency for different throat angle

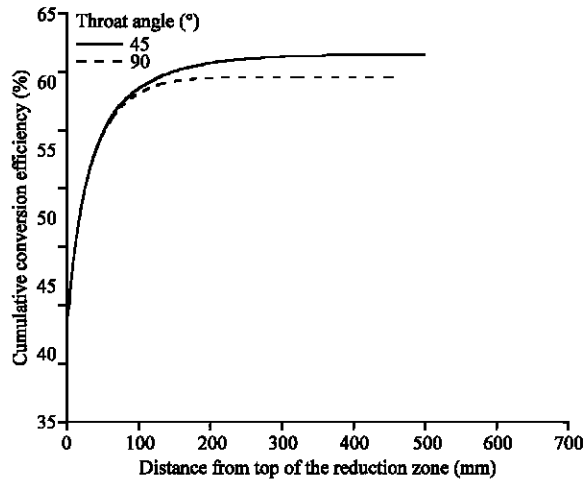


Fig. 7: Axial variation of cumulative conversion efficiency for different throat diameter

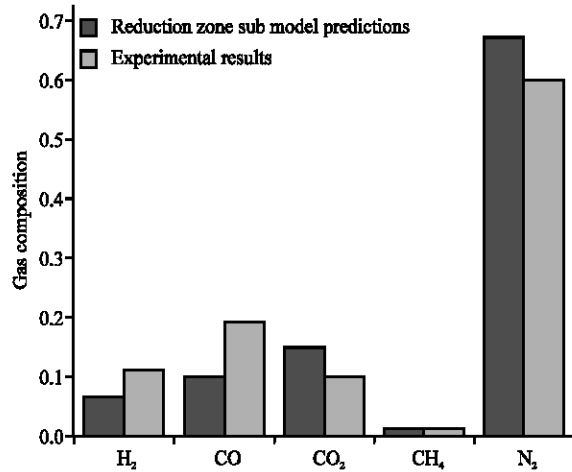


Fig. 8: Model comparison with experimental data of Jayah *et al.* (2003)

throat diameters (30 cm) decrease the cumulative conversion efficiency, because the latter decreases the temperature due to the divergent effect and hence the reaction rate. Although smaller throat diameter increase the cumulative conversion efficiency, it also needs a longer gasification.

VALIDATION OF REDUCTION ZONE SUB MODEL

Reduction zone sub model predictions are compared with the Experimental data reported by Jayah *et al.* (2003) (Fig. 8). Composition of producer gas is compared and shown in Table 3. Experimentally reported compositions

Table 3: Model comparison with experimental data of Jayah *et al.* (2003)

Gas compositions	Reduction zone sub model	Experimental results (Jayah <i>et al.</i> 2003)
H ₂	0.068	0.110
CO	0.101	0.190
CO ₂	0.150	0.100
CH ₄	0.012	0.013
N ₂	0.671	0.600

Table 4: Analysis of cumulative conversion efficiency for different parameters

Moisture content	15								
Wood diameter (cm)	1			4			6		
Air temp. (K)	300	400	600	300	400	600	300	400	600
Cumulative efficiency at exit (%)	62.3	621.5	61.0	60.2	60.50	61	58.8	58.9	59.5
Moisture content	20								
Wood diameter (cm)	1			4			6		
Air temp. (K)	300	400	600	300	400	600	300	400	600
Cumulative efficiency at exit (%)	61	61.3	61.8	59	59.3	59.8	57.7	59	58.4
Moisture content	15								
Wood diameter (cm)	1			4			6		
Air temp. (K)	300	400	600	300	400	600	300	400	600
Cumulative efficiency at exit (%)	60	60.2	60.7	58	58.3	58.8	56.7	57	57.4

are for air flow rate of 55.6 kg h⁻¹, wood rate of 18.6 kg h⁻¹ and wood moisture rate of 3.4 kg h⁻¹. These values are used to predict the gas compositions and compared with experimental data, the cumulative conversion efficiency for various parameters also listed in Table 4. Table 4 shows that compositions of all components are in good agreement with experimentally reported data.

CONCLUSION

The modeling of a reduction process in a down draft gasifier is performed. From the analysis for the effect of moisture content, preheating of air, wood diameter, throat angle, throat diameter, following conclusions are drawn.

- An increasing fuel moisture content causes the feedstock cumulative conversion efficiency to drop. A longer reduction zone is necessary to achieve the same fractional biomass conversion as the moisture content increases. If wood chips are given sufficient sun exposure, the moisture content can be reduced to around 15% which gives a cumulative conversion efficiency of 61%.
- Wood diameter is found to have a significant effect on the required length of the reduction zone for complete gasification as well as on conversion efficiency. For the reduction zone length of 280 mm, the cumulative conversion efficiency is found to be 56% for 6 cm wood diameter. If the size is reduced to 4 cm, the cumulative conversion efficiency increases by 2%.
- High inlet air temperature is found to be beneficial for gasifier performance but the improvement in conversion efficiency does not seem to be commensurate with the penalties associated with preheating. However, if the temperature of inlet air can be increased by an external means such as waste heat from factories, it can be beneficial in the way of improved conversion efficiency of the plant.
- The result of the modeling has been used to optimize the length of the gasification zone for effective gasification process. The effective reaction takes place over a length of 280 mm of the reduction zone only. After 280 mm of the zone, the cumulative conversion efficiency remains same, whereas the temperature of the gas gets reduced from 1250 K to 700 K because of the wall heat transfer and the outside convection environment.

NOMENCLATURE

B and S	= Condition at the bulk fluid and particle surface
C _c	= Average particle carbon concentration
C _g	= Total concentration (kg mole m ⁻³),
C _p	= Fluid specific heat
D _{an}	= Molecular diffusivity of component a to the mixture
ε _b	= Bed void fraction
G	= Superficial mass velocity,
H	= Heat transfer coefficient between the bulk and the particle.
H _g	= Enthalpy flux of gases,
H _s	= Enthalpy flux of solid,
K	= Thermal conductivity.
K _m	= Fluid thermal conductivity of the gas mixture
K _M	= Mass transfer coefficient,

M	= Molecular weight
M _i	= Viscosity of pure component I, a function of mixture temp and total pressure
M _j	= Viscosity of complete mixture
N _g	= Total mole flux (kmole m ⁻² sec ⁻¹),
P	= Total pressure
P _r	= Prandtl No.
V _g	= Superficial velocity (m sec ⁻¹),
R	= Ideal Gas constant,
Re	= Reynolds No.
r _o	= Particle radius at any gasification zone location
r _p	= Initial particle radius
Sc	= Schmidt No.,
T _g	= Temperature and
V _p	= Particle volume and
Y	= Mole fraction of components,
ws	= Amount of equilibrium shift, (kg kmol ⁻¹)
μ _m	= Fluid viscosity
ρ	= Fluid density.
ΔH ₃	= Heat of water-gas shift reaction

REFERENCES

- Chen, J.S., 1987. Kinetic engineering modelling of co-current moving bed gasification reactors for carbonaceous material. Ph.D Thesis, Cornell University, New York.
- Colburn, A.E., 1931. Heat transfer and pressure drop in empty, baffled and packed tubes, I-Heat transfer in packed tubes. *Ind. Eng. Chem.*, 23: 910-913.
- Eckert, E.R.G., 1956. Engineering relations for heat transfer and friction in high-velocity laminar and turbulent boundary-layer flow over surfaces with constant pressure and temperature. *Trans. Am. Soc. Mech. Eng.*, 78: 1273-1283.
- Goodridge, E. and H.H. Quazi, 1967. The water-gas shift reaction: A comparison of industrial catalysts. *Trans. Inst. Chem. Eng.*, 45: T274-279.
- Groeneveld, M.J. and W.P.M. Van Swaaij, 1979. Gasification of solid waste--potential and application of co-current moving bed, gasifiers, *Applied Energy*.
- Iyer, P.V.R., T.R. Rao, P.D. Groover and N.P. Singh, 2002. Biomass-thermochemical characterization. Chemical Engineering Department, Indian Institute of Technology, Delhi, pp: 9-16.
- Jayah, T.H. Lu Aye, R.J. Fuller and D.F. Stewart, 2003. Computer simulation of a downdraft wood gasifier tea drying. *Biomass. Biol. Energy*, 25: 459-469.
- Milligan, J.B., 1994. Downdraft Gasification of Biomass. Ph.D Thesis, Aston University Birmingham, UK.

- Parikh, P.P., A.G. Bhave, D.V. Kapse and Shashikantha, 1989. Study of thermal and emission performance of small gasifier-dual-fuel engine systems. *Biomass*, 19: 75-97.
- Perry, R.H., D.W. Green and J.O. Maloney, 1984. *Perry's Chemical Engineers' Handbook*. 6th Edn. McGraw-Hill, New York.
- Petrovic, L.J. and G. Thodos, 1968. Mass transfer in the flow of gases through packed beds. *Ind. Eng. Chem. Fundam.*, 7: 274-80.
- Reed, T.B. and A. Das, 1988. *Handbook of biomass downdraft gasifier engine system*. Golden, CO: SERI.
- Sherwood, T.K., R.L. Pigford and C.R. Wilke, 1975. *Mass Transfer*. McGraw-Hill, New York.
- Wilke, C.R., 1950. Diffusional Properties of Multicomponent Gases. *Chem. Eng. Progr.*, 46: 95-104.
- Yoon, H.Y., J. Wei and M.M. Denn, 1978. A model for moving bed coalgasification reactors. *AIChE. J.*, 24: 885-903.
- Zainal, Z.A. Ali Rifau, G.A. Quadir and K.N. Seetharamu, 2002. Experimental investigation of a downdraft biomass gasifier. *Biomass Bioenergy*, 23: 283-289.